The citation is:

Mustafa, A., Bruwier, M., Archambeau, P., Erpicum, S., Pirotton, M., Dewals, B., Teller, J., 2018. "Effects of spatial planning on future flood risks in urban environments." *Journal of Environmental Management* 225, 193–204. https://doi.org/10.1016/j.jenvman.2018.07.090

Effects of spatial planning on future flood risks in urban environments

Abstract: Urban development may increase the risk of future floods because of local changes in hydrological conditions and an increase in flood exposure that arises from an increasing population and expanding infrastructure within flood-prone zones. Existing urban land use change models generally consider the expansion process and do not consider the densification of existing urban areas. In this paper, we simulate 24 possible urbanization scenarios in Wallonia region (Belgium) until 2100. These scenarios are generated using an agent-based model that considers urban expansion and densification as well as development restrictions in flood-prone zones. The extents of inundation and water depths for each scenario are determined by the WOLF 2D hydraulic model for steady floods corresponding to return periods of 25, 50, and 100 years. Our results show that future flood damages and their spatial distributions vary remarkably from one urbanization scenario to another. A spatial planning policy oriented towards strict development control in flood-prone zones leads to a substantial mitigation of the increased flood damage. By contrast, a spatial planning policy exclusively oriented to infill development with no development restrictions in flood-prone zones would be the most detrimental in terms of exposure to flood risk. Our study enables the identification of the most sensitive locations for flood damage related to urban development, which can help in the design of more resilient spatial planning strategies and localize zones with high levels of flood risk for each scenario.

Keywords: urban flooding; flood damage; urban expansion; urban densification; agent-based model; Wallonia.

1. Introduction

The magnitude and frequency of floods, particularly river floods, are currently increasing in northwest Europe (Moel and Aerts, 2010). Climate change and urban development are key elements contributing to increased flood damage (Poelmans et al., 2011). Urbanization increases the damage due to flood exposure caused by the increasing population and infrastructure within flood-prone zones. In addition, transforming natural surfaces into artificial surfaces causes an increase in flooding frequency because of poor infiltration (Huong and Pathirana, 2013). Recent studies have shown different effects of climate change and urban development on flood risk (e.g., Löschner et al., 2017). The Intergovernmental Panel on Climate Change claimed, with low confidence, that climate change has affected the frequency and magnitude of flooding (IPCC, 2014). Poelmans et al. (2011) and Beckers et al. (2013) investigated the relative impact of both climate change and future urban expansion on floods. Poelmans et al. (2011) found that the potential flood-related damage was mainly influenced by urbanization on the floodplains. Similar results were obtained by Beckers et al. (2013) in a "dry" climate scenario, while climate change is more influential in a "wet" scenario. Hannaford (2015) found that changes in peak flows could not be directly attributed to climate change across the United Kingdom. Cammerer et al. (2013) analyzed potential changes in future flood exposure because of different land use developments and found that the range of potential changes in flood-exposed residential areas varies from no further change to 159% increase depending on the spatial planning scenarios.

Previous studies that coupled urban development scenarios with hydrological models using a spatial resolution between 50 m and 100 m (e.g., Beckers et al., 2013; Cammerer et al., 2013; Poelmans et al., 2010; Tang et al., 2005) considered only urban expansion processes, i.e., transitions from nonurban to urban land use. Such a binary process may fail to estimate the damage related to floods properly because it neglects the different densities of urban cells and the variation in density over time. Some studies used vector data for small urban areas (e.g., Achleitner et al., 2016). However, the drawback of using such a vector data is that it requires intensive computational resources to simulate future urbanization in larger study areas such as regions.

This study investigates the possibility of flood damage related to different urban development scenarios in Wallonia region (Belgium) if there is no further climate change. The main contribution of our study is the evaluation of the impacts on flood damages from spatial planning policies that consider expansion versus densification processes compared with spatial planning policies oriented towards development restrictions in flood-prone zones.

2. Materials and Methods

2.1. Study area

Wallonia covers an area of 16,844 km^2 in southern Belgium (Figure 1). Its hydrographic network is structured along four hydrographic districts (Meuse, Rhine, Escaut Scheldt or Seine basin), 15 hydrographic subbasins and 6,208 so-called PARIS sectors, each of which corresponds to a river stretch with relatively homogeneous characteristics in the main riverbed and in the floodplains. In this study, we only consider the two main districts of Meuse and Escaut, which cover 73% and 22% of Wallonia, respectively. The areas of most subbasins in the Meuse district are larger than in the Escaut district, while the population density is generally lower in the former. The Meuse aval subbasin is the largest in Wallonia and the most densely inhabited in the Meuse district. Four subbasins in the Meuse district have a population density lower than 100 inhabitants/km^2, while it is higher than 175 inhabitants/km^2 for all subbasins in the Escaut district (DGO3 2015a, 2015b). The Meuse district is mainly covered by agricultural uses and forests. The average annual precipitation ranges between 1,000 and 1,400 mm and snowmelt may influence flood discharges in some parts of the Meuse district. The Escaut district is mainly covered by agriculture and built-up uses. The average annual precipitation in the Escaut district is between 700 and 850 mm. In both districts, high flows generally occur in winter and low flows in summer, following the rainfall–evaporation regime.

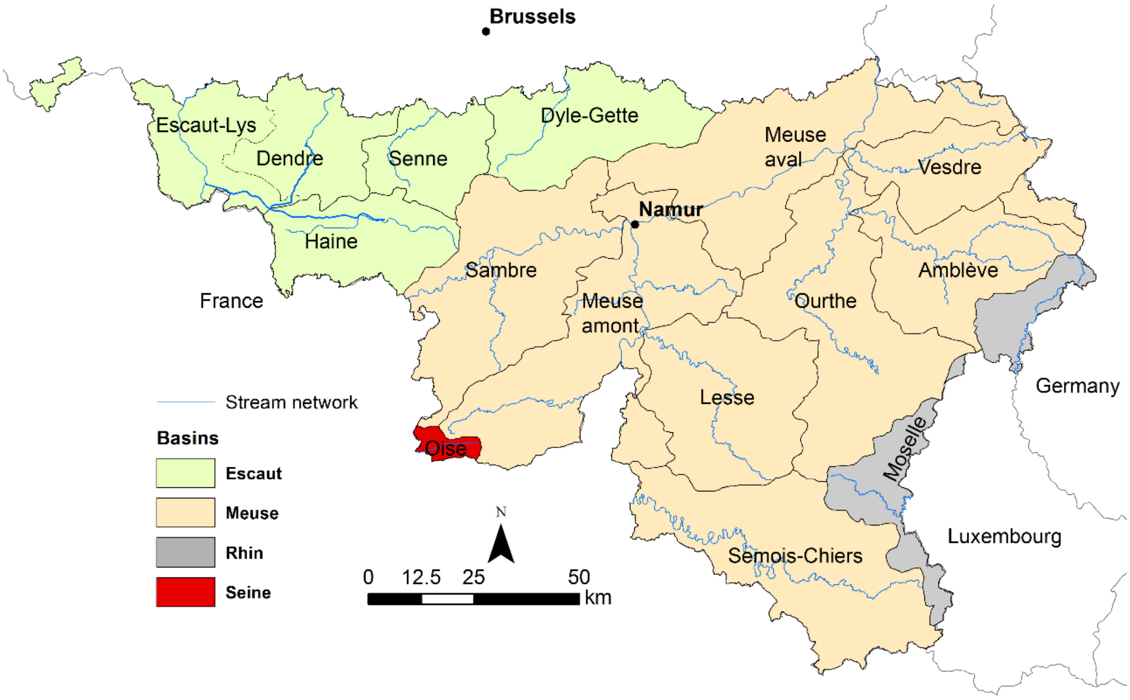

Figure 1: *The four hydrographic districts and 15 hydrographic subbasins in Wallonia (Belgium).*

2.2. Methodology

Our methodology to assess flood damage for different urbanization scenarios consists of three main steps (Figure 2). Firstly, urban land use data for 1990, 2000 and 2010 were generated based on Belgian cadastral data. Thereafter, future urbanization scenarios were simulated for 2030, 2050, 2070, and 2100 by extrapolating the observed demand rates for urban development. New urban cells were then allocated using a spatial agent-based model (ABM). Secondly, inundation maps were computed for flood discharges with the WOLF 2D hydraulic model (Bruwier et al., 2015; Ernst et al., 2010). Thirdly, the future urbanization maps were combined with the computed inundations maps to evaluate the flood damage for each future urbanization scenario using a flood loss estimation model (FLEMO).

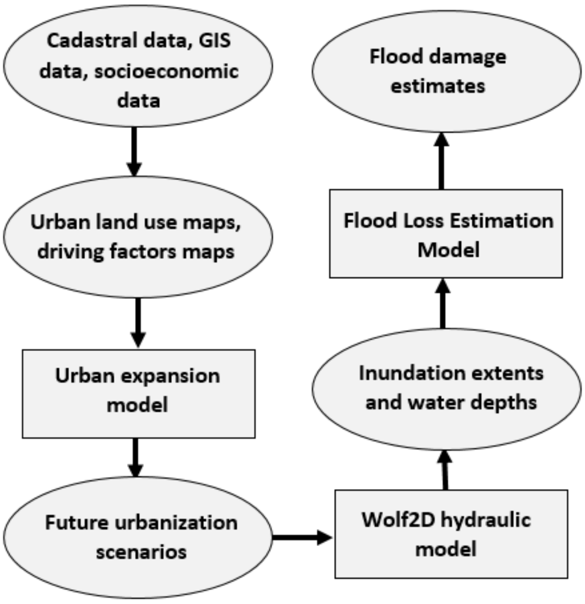

Figure 2: Flowchart explaining the methodological structure

2.2.1. Future urbanization scenarios

Data

Urban land use data for 1990, 2000, and 2010 were generated as 100 m ×100 m raster grids to show the spatial distribution of urban density. The Belgian Cadastral Database (CAD) provided by the Land Registry Administration of Belgium was used to generate urban land use data following the methodology detailed in Mustafa et al. (2018a). The urban density indices were classified into six density classes (Table 1) using the natural breaks technique (Jenks and Caspall, 1971). In the observed data from 2010, about 80% of urban land is related to very-low-density urban classes (classes 1 and 2), whereas only 6% are highly dense areas (Table 1), which indicates a strong potential for the density of existing urban areas to be increased.

Table 1. Urban density classes.

Class	Minimum*	Maximum*	Walloon coverage	Fraction of built-up area
Class-0 (non urban)	0	1%	83.5%	-
Class-1 (lowest-density)	1%	5.8%	7.6%	46%
Class-2	5.8%	13.8%	5.4%	33%
Class-3	13.8%	26.1%	2.5%	15%
Class-4	26.1%	48.6%	0.8%	5%
Class-5 (highest-density)	48.6%	100%	0.2%	1%

*urban coverage range (minimum to maximum) for each cell of 100 m × 100 m.

Agent-based model

Agent-based model (ABM) is a common land use change modeling approach, because it offers a way to incorporate the influence of human decision-making on land use change dynamics considering social interactions, adaptation, and decision-making at different levels (Matthews et al., 2007).

We introduce an ABM, inspired by the work of Mustafa et al. (2017) in allocating the necessary new urban developments. The ABM simulates two development processes: expansion (transitions from nonurban density to urban densities) and densification (transitions from lower to higher urban densities). Several urbanization driving forces were operationalized and included in the model. Table 2 lists the drivers considered in this research , which were chosen based on the findings from previous studies regarding urbanization in Wallonia (e.g., Mustafa et al., 2018a, 2018b). This study distinguishes large (population ≥ 90,000) from medium-sized cities (population ≥ 20,000 and < 90,000). The regional zoning plan, which is commonly called the *plan de secteur* (PdS) in Wallonia, defines authorized land uses for each part of the territory. A residential or industrial category was assigned to each cell based on the current PdS. In addition, it considers possible urban development restrictions in flood-prone zones.

Table 2: Selected built-up driving factors. All data were resampled to the same cell resolution of 100 m × 100 m.

Factor	Name	Type	Unit
E	Elevation (DEM)	Continuous	Meter
S	Slope	Continuous	Percent rise
DR1	Dist. to Road1 (highways)	Continuous	Meter
DR2	Dist. to Road2 (main roads)	Continuous	Meter
DR3	Dist. to Road3 (secondary roads)	Continuous	Meter
DR4	Dist. to Road4 (local roads)	Continuous	Meter
DRS	Dist. to railway stations	Continuous	Meter
DLC	Dist. to large-sized cities	Continuous	Meter
DMC	Dist. to medium-sized cities	Continuous	Meter
EMP	Employment rate	Continuous	Percent
WI	Wealth index	Continuous	Percent

The agents are categorized into three groups with different characteristics and goals (Figure 3): i.e., developer (DevAG), existing resident (ExtAG) and planning permission authority (PPA). At each time step, corresponding to one year, several DevAGs consider global and local factors in selecting locations for development. Each DevAG determines the transition potential from one class to another for a location according to the following equation:

$$UF_{DevAG} = \left(P_c\right)_{ij} \times \left(P_n\right)_{ij}^{\sigma} \tag{1}$$

where UF_{DevAG} is the utility function for DevAG, P_c is the transition potential for cell *ij* from one urban class to another according to a set of accessibility, geophysical and socioeconomic factors, P_n represents the DevAG's neighborhood preferences, and σ is a variable representing the relative importance of the neighborhood preferences.

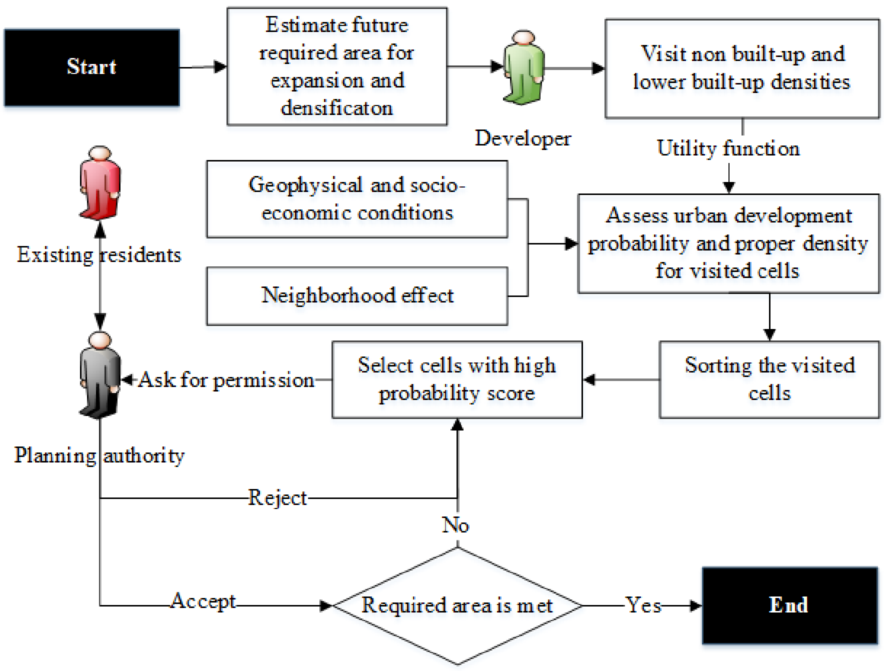

Figure 3: *The overall framework of the agent-based model. Three agents groups are proposed: developers, existing residents, and planning permission authority. Planning authority interacts with developers and existing residents to determine the new locations to develop or densify.*

The P_c is determined according to the following equation:

$$(P_c)_{ij} = a_{AG} \times E + b_{AG} \times S + c_{AG} \times DR1 + d_{AG} \times DR2 + e_{AG} \times DR3 + f_{AG} \times DR4 + g_{AG} \times DRS + h_{AG} \times DLC + i_{AG} \times DMC + j_{AG} \times EMP + k_{AG} \times WI \quad (2)$$

where a_{AG} to p_{AG} are specific weights assigned to utility function factors listed in Table 2. The P_n is dynamically computed at each time-step using an embedded cellular automata model according to the method proposed by White and Engelen (2000).

After the respective DevAG has selected a cell to develop or densify and at which density, the PPA must be asked to grant permission to develop the cell. The PPA gives permission for the development according to two factors: (i) land use zoning regulations, and (ii) the resistance of existing residents against the proposed new development. Three zone categories are set by the PPA: (1) permitted (legal urban zones); (2) severely restricted (arable lands, grasslands, forests, and other classes); and (3) forbidden (water bodies) according to the authorized zoning plan. If a cell is located in a permitted or in a forbidden zone, PPA will instantaneously accept or reject the permission respectively. Otherwise, if the cell is located in a severely restricted zone, PPA will give permission for a specific percentage of the change amount (allowed rate) for each time step as follows:

$$PPAZ = \begin{cases} accept, & Dt \leq ARt \\ refuse, & otherwise \end{cases} \quad (3)$$

where *PPAZ* is the PPA's decision on a development proposal for a cell within severely restricted zones, *Dt* is the developed cells within severely restricted zones in time-step *t* and *ARt* is the allowed rate. Second, the PPA considers concerns of the local residents as follows:

$$PPADec = \begin{cases} accept, & AvDt_k \leq AcD_k \\ refuse, & otherwise \end{cases} \quad (4)$$

where *PPADec* is the PPA's final decision, $AvDt_k$ the average density at time-step *t* for a 3×3 neighborhood window in which a density class *k* occupies ≥ 50% of the total cells within the neighborhood window, and AcD_k is the accepted average density value for a neighborhood with a density *k*.

The model is calibrated with urban development that was observed between 1990 and 2000. The calibration results are then used to validate the model with the development between 2000 and 2010. A genetic algorithm (GA) is used to calibrate the model parameters. The GA is one of the recent methods used to calibrate land use change models (e.g., García et al., 2013). To set the operators values for the GA, we performed a number of empirical experiments on different values of the operators and selected the best ones, following Mustafa et al. (2018a). The GA's objective function is detailed in Mustafa et al. (2018a).

Urbanization scenarios

A set of 24 different urbanization scenarios were generated (Table 3). The estimates of quantity uncertainty are commonly based on the simulation of different scenarios according to any assumption of extrapolation from the past quantity of changes, demographic growth, or socioeconomic transitions (e.g. Cammerer et al., 2013; Poelmans et al., 2010). Using linear extrapolations of the observed expansion and densification rates between 1990, 2000 and 2010 in Wallonia, three change rates are proposed for the future: low- (rate between 2000 and 2010), medium- (rate between 1990 and 2010), and high-demand (rate between 1990 and 2000).

Table 3: 24 future urbanization scenarios that vary in the demand rate for new developments (three scenarios) and spatial planning policies.

	Urbanization rate Ban on new developments	High (1990-2000)	Medium (1990-2010)	Low (2000-2010)
Business as usual (BAU)	None	Scenario1	Scenario2	Scenario3
	In zone 3	Scenario4	Scenario5	Scenario6
	In zones 2 and 3	Scenario7	Scenario8	Scenario9
	In all zones	Scenario10	Scenario11	Scenario12
Densification	None	Scenario13	Scenario14	Scenario15
	In zone 3	Scenario16	Scenario17	Scenario18
	In zones 2 and 3	Scenario19	Scenario20	Scenario21
	In all zones	Scenario22	Scenario23	Scenario24

Regarding the DevAG's behavior when selecting specific land to develop (allocation uncertainty), we used the Time Monte Carlo method, proposed by Mustafa et al. (2018c).

The spatial planning policies considered in this research are: i) urban development restriction in flood-prone zones and ii) densification with or without expansion.

We consider three zones represented in the official flood-prone maps:

- zones of "low flood hazard," referred to hereafter as "zone 1";
- zones of "medium flood hazard," referred to hereafter as "zone 2";
- zones of "high flood hazard," referred to hereafter as "zone 3."

Based on these three flood-prone zones, four urban development restriction scenarios are considered: no restriction, restrictions in flood-prone zone 3, restrictions in flood-prone zones 2 and 3, and restrictions in all flood-prone zones.

The business-as-usual (BAU) scenarios are in line with recent urbanization trends considering the share of expansion versus densification dynamics. In the densification scenarios, we assume that the expansion process is blocked and the required new areas for expansion are taken from the next density levels. For instance, the expansion from class 0 to classes 1 and 2 is substituted by densifying the same area from class 1 to class 2. In cases where the available area of a specific class is not sufficient to be further densified, the model densifies cells from the next density class. After simulating each density class, the model assigns an urban use (residential or industrial) for each cell according to the current zoning plan.

2.3. Hydrological characteristics

The computation of inundation extents and water depths for the generation of flood hazard maps in Wallonia was performed for steady flows corresponding to return periods of 25, 50 and 100 years, using the 2D hydraulic model, WOLF 2D, with a cell size of 5 m × 5 m.

In this study, we only consider the water depth to determine the flood damage. Flood damage is influenced by additional factors such as the flow velocity, the flood duration, transport of sediments, and early warning. In this study, however, flow velocity remained low, which is typical in floodplains of lowland rivers. Therefore, it has a negligible influence on the damage (Kreibich et al., 2009; Pistrika and Jonkman, 2010). We use stage-damage functions, which were developed for relatively long-duration floods , which is consistent with the flood events of interest in this study. Water depth is widely recognized as the factor with the greatest influence on flood damage estimation (Büchele et al., 2006; Kreibich et al., 2009; Merz et al., 2007). The specific contribution of additional factors remains incompletely understood and there is no generally accepted procedure exists for quantifying their influence in large-scale damage modelling as undertaken in this study.

Maps of inundation extents and water depths were computed for several hundreds of kilometers of rivers throughout Wallonia (Figure A-1 in the Appendix). In the Escaut district, only a limited portion of all sectors was computed, except for the Escaut-Lys subbasin where results are available all along the Scheldt river (Escaut). No river was computed in the Haine subbasin. In the Meuse district, computations were performed all along the rivers Amblève, Meuse, Ourthe, Sambre, Vesdre, and Viroin rivers. In the Lesse and Semois-Chiers subbasins, results are only available for some reaches of the Lesse and Semois rivers.

2.4 Flood damage assessment

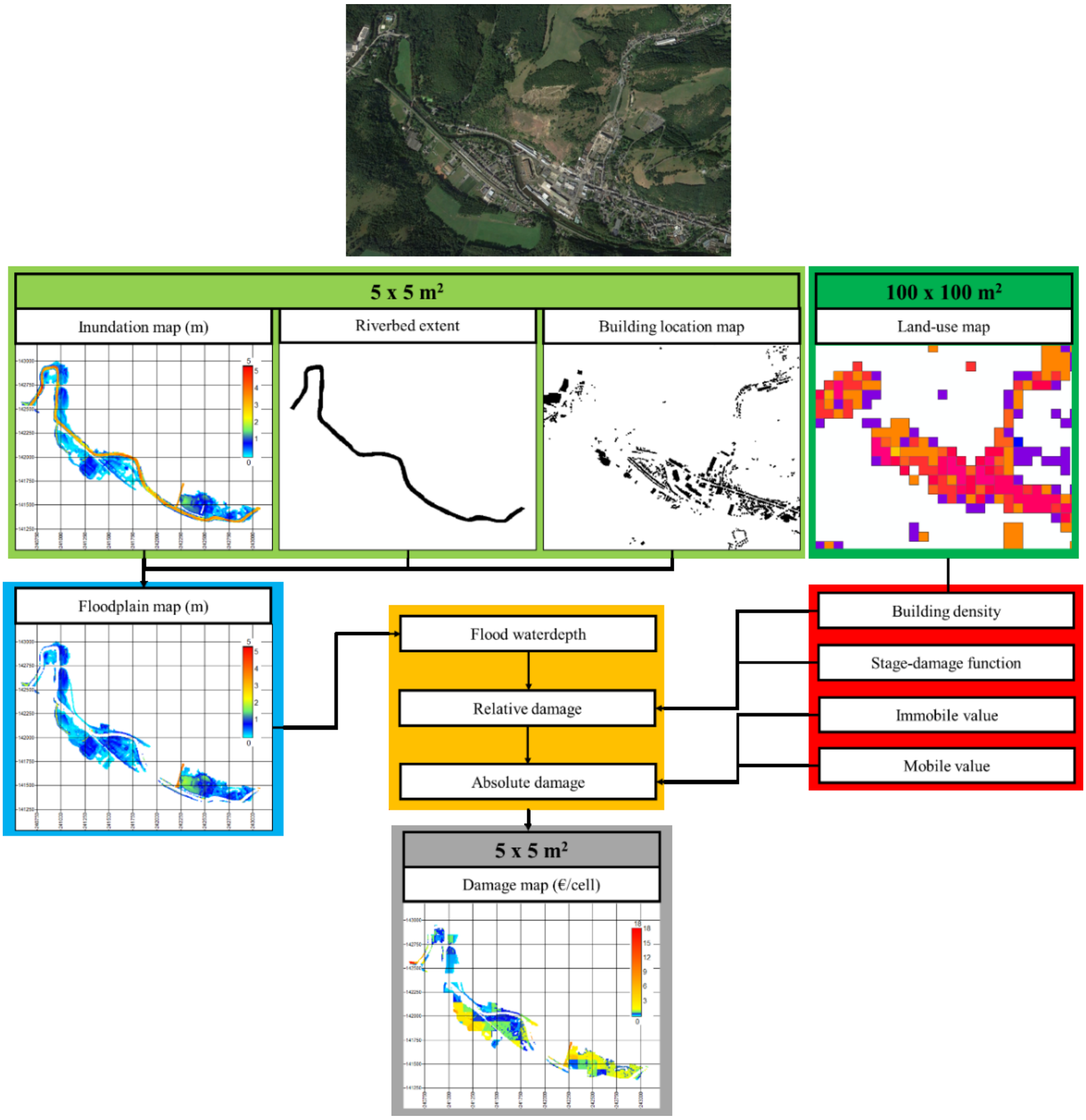

Figure 4: The methodology for estimating the flood damage. The relative damage is computed using the urban maps, and the appropriate stage-damage function. The absolute damage is then derived from the relative damage using mobile and immobile values of the elements.

The land use class of each floodplain cell was determined from the land use map at a resolution of 100 m^2. The ABM considers two land uses: residential and industrial. Only damages related to buildings are computed in this study and we do not consider damages related to other land uses like infrastructure, agriculture, and forests.

The susceptibility of a building to flooding was assessed by a stage-damage function giving the relative damage, i.e., the share of the total value of a building that is damaged by the flood, as a function of the water depth. In this study, we used the stage-damage functions for residential and industrial categories defined by the FLEMO (Kreibich et al., 2010) (Fig. 4). The damage assigned to residential and industrial buildings is split between mobile and immobile assets (Figure A-2 in the Appendix).

The determination of flood damage in monetary value requires the assignment of a specific value to the buildings. In our study, the monetary values of residential and industrial buildings were chosen so that in the baseline scenario, the estimated flood damages are similar to those computed by Beckers et al. (2013) along the Meuse river for a 100-year flood. We used identical monetary values for both residential and industrial categories and assume that immobile values are four times higher than mobile ones, which respects the ratios proposed by Beckers et al. (2013). In Table 3, the resulting immobile and mobile values are significantly higher than the values used by Beckers et al. (2013). These results were obtained from the type of elements for which the monetary values are assigned: i.e., parcels for Beckers et al. (2013) and buildings in our study.

Table 3: Prices of the residential and industrial categories.

	Beckers et al. (2013)		The present study	
Elements at risk	Parcel		Building	
	Immobile	Mobile	Immobile	Mobile
Residential	389 €/m^2	119 €/m^2	2000 €/m^2	500 €/m^2
Industry	343 €/m^2	90 €/m^2	2000 €/m^2	500 €/m^2

The United Nations defines risk as the combination of the probability of an event to occur and its negative consequences (UNISDR, 2009). In this study, an indicator of the flood risk is computed as the expectation value of damage for the three return periods T_{25}, T_{50}, and T_{100} following Ernst et al. (2010). This indicator is used for the determination of the impact of urbanization on flood damage with a single scalar value representative of the damage occurring in between the three return periods considered in this study.

3. Results and discussion

3.1. Influence of the number of urban density classes

The sensitivity of the computed flood damage to the number of urban density classes was assessed for flood discharges Q_{25} and Q_{100}. We examined 1 to 8 density classes for each land use category, the flood damage D_d computed with d classes of density is compared to the results obtained with the highest number of classes, i.e. D_9, using the following relative difference E_d:

$$E_d = \frac{D_d - D_9}{D_9} \quad (5)$$

The computed flood damages are overestimated by 48% to 105% when a single class of urban density is used (Figure 5). When the number of classes is increased, the value of the computed flood damage converges rapidly towards values close to D_9, and fluctuates slightly around this value. When five classes of densities are used, the relative error remains lower than 5% for the two flood discharges Q_{25} and Q_{100}. Beyond this number of classes, the relative difference E_d does not seem to decrease significantly.

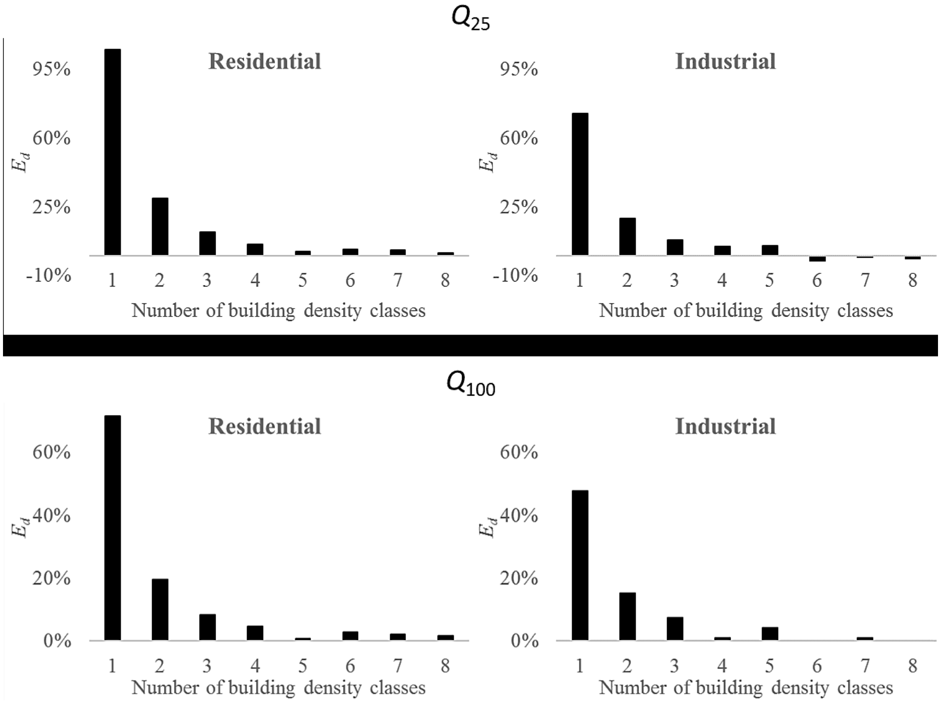

Figure 5: Sensitivity of the total flood damage computed with different numbers of classes of urban density, for flood discharges Q25 and Q100.

Therefore, we used five classes of density for each land use category (i.e., residential and industrial). This sensitivity analysis confirms the importance of considering different levels of urban density when assessing flood damage. Considering urbanization as a binary process (i.e., urban vs. nonurban) may lead to a severe miscalculation of flood damage in both magnitude and location.

3.2 Future urban patterns

The proposed ABM generates a series of future possible urbanization scenarios. The validation of the model, simulated 2010 vs observed 2010 map, shows a comparable results to those reported in the literature (e.g., Han and Jia, 2016; Long et al., 2013; Wang et al., 2013) with Kappa indices of 0.88, 0.87, 0.90, 0.92 and 0.92, for classes 1-5 respectively.

The observed urban density class to class changes suggest that transitions from class 1 to classes 4 and 5, class 2 to class 5, and class 3 to class 5 over the study period are marginal. Therefore, we set the densification as the transitions from class 1 to classes 2 and 3, from class 2 to classes 3 and 4, from class 3 to class 4, and from class 4 to class 5.

Figure 6 illustrates the future urbanization maps for 2030 and 2100 for scenarios 1 and 13 (Table 3). In scenario 1 (BAU), the development of new low and medium density lands occur continually and therefore Wallonia will experience a fragmented urban landscape in the future. In scenario 13 (densification), there are sufficiently low and medium density urban areas that can accommodate future urbanization. As mentioned, we assumed the required new areas for expansion are taken from the next density class. Consequently, the area of class-1 and class-2 will decrease over time. Figure A-3 (Appendix) shows the percentage of change for each class when compared with the 2010 observed urban pattern.

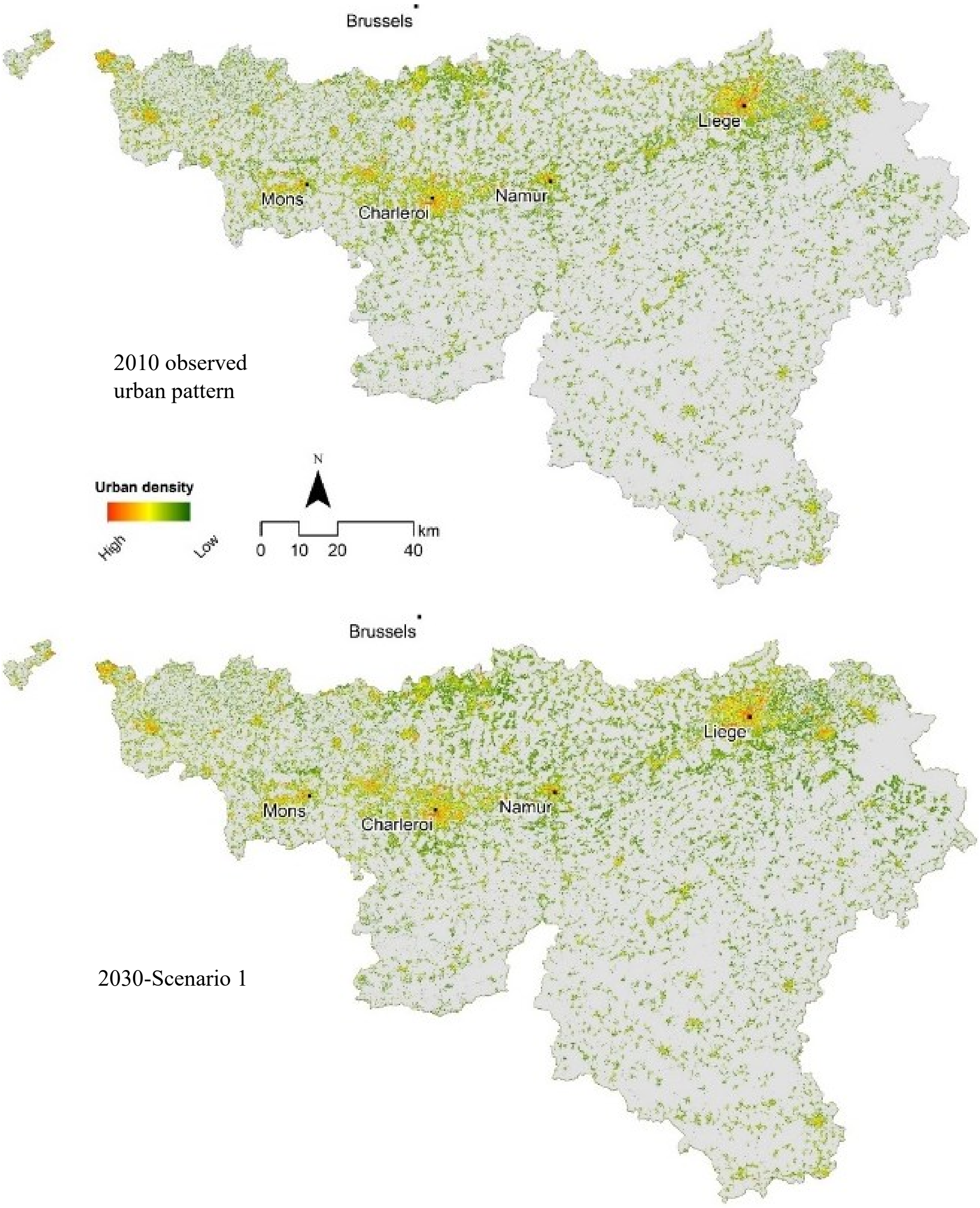
Brussels
Liege
Mons
Charleroi
Namur
2010 observed
urban pattern
Urban density
High
Low
N
0 10 20 40
km
Brussels
Liege
Mons
Charleroi
Namur
2030-Scenario 1

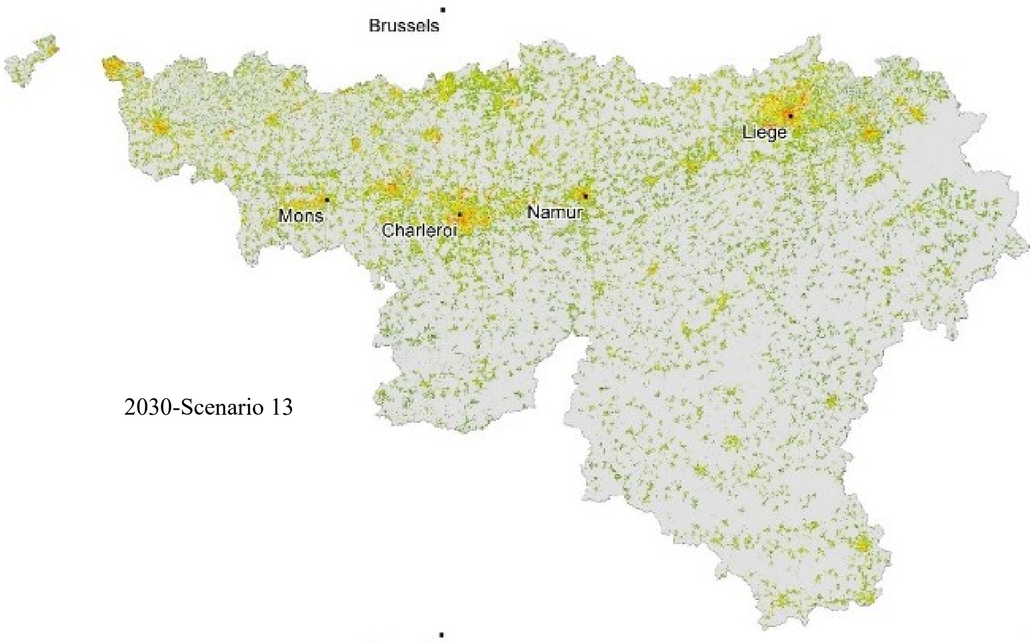
Brussels
Liege
Mons
Charleroi
Namur
2030-Scenario 13

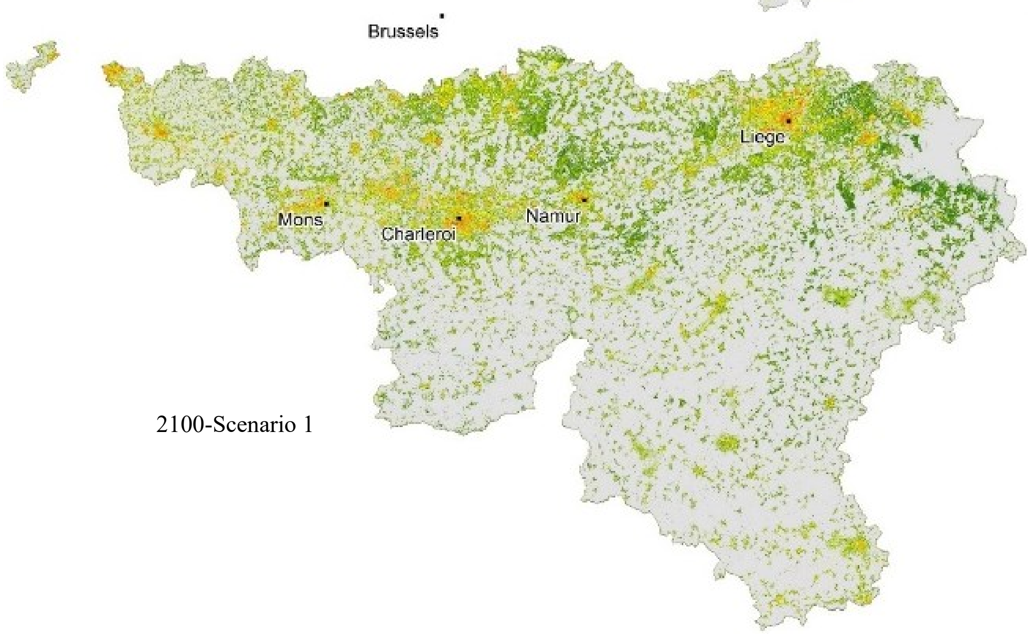
Brussels
Liege
Mons
Charleroi
Namur
2100-Scenario 1

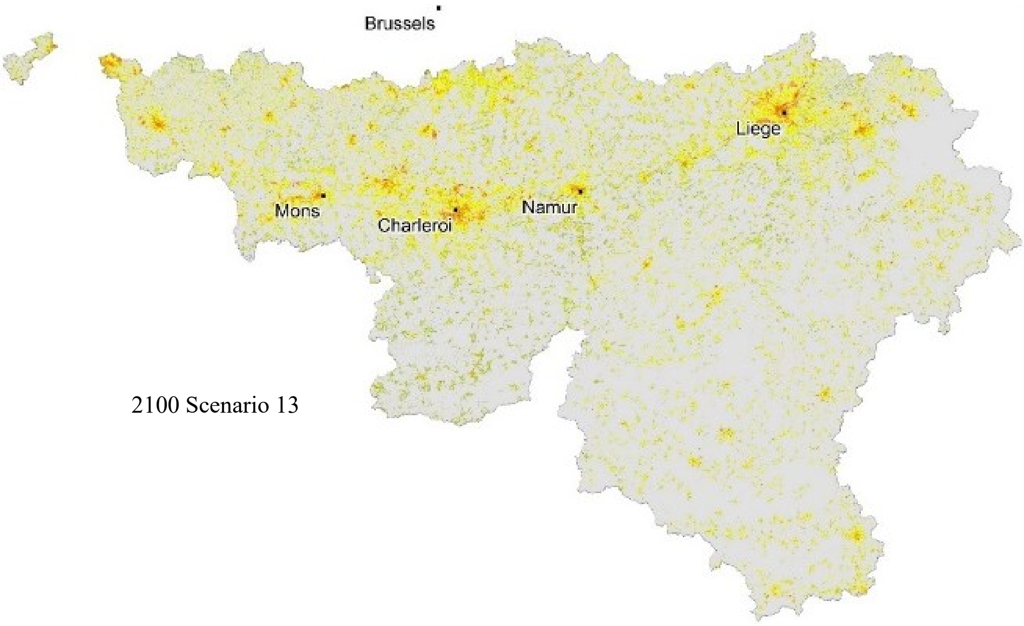

Figure 6: *Future urbanization maps for 2030 and 2100 for 2030 and 2100 for scenarios 1 and 13 (Table 3).*

3.3 Flood risk

We present a comparison between the flood risk indicators computed for the baseline scenario (observed 2010) and the different subbasins in section 3.3.1. Section 3.3.2 investigates the influence of the uncertainty of urbanization scenarios on the results of the risk computation. Finally, we quantify the increase in future flood risk indicator due to urbanization up to 2100 in section 3.3.3.

The uncertainty in the computation of the flood risk indicator resulting from the adopted resolution of the land use data (100 m × 100 m) is expected to be significant, particularly for moderate events with limited flood extents such as the Q_{25} flood discharge. Consequently, the assessment of the flood risk in absolute monetary values should be interpreted with caution. Following Moel and Aerts (2010), we therefore use relative values of flood risk, taken as a percentage of a reference risk values (in the baseline scenario) computed with the same methodology.

3.3.1 Distribution of the flood risk indicator between the sub-basins in the baseline scenario

Figure 7 illustrates the relative contributions of different subbasins to the flood damages for the Q_{25}, Q_{50}, and Q_{100} flood discharges (445×10^6 €, 620×10^6 € and 830×10^6 €, respectively) and to the value of the flood risk indicator (18×10^6 €). For most subbasins, the relative contributions are very similar for the different flood discharges as well as for the flood risk indicator. The variations between these are the highest for the Meuse aval subbasin in which the contribution to the overall flood damages varies between 14% and 20% depending on the considered flood discharge. In what follows, we only discuss the flood risk indicator because very similar trends were obtained for the flood damages corresponding to the three computed flood discharges.

The results show that:

- the *Meuse amont*, *Meuse aval* and *Ourthe* subbasins have the highest contribution to the computed flood risk indicator. This is consistent with the high number of sectors that are computed in these subbasins (Figure A-1).
- The flood risk indicator in the *Vesdre* subbasin is more than twice as high as in the *Semois-Chiers*, *Lesse*, and *Amblève* subbasins, despite a smaller subbasin area and the existence of large reservoirs in the upper part of the *Vesdre* catchment. This is certainly related to the population density, which is four to six times higher in the *Vesdre* subbasin than in the others.
- In the *Escaut* district (*Dyle-Gette*, *Senne*, *Dendre* and *Escaut-Lys* subbasins), the computed flood risk indicator is the lowest because only a limited number of sectors are computed (Figure A-1).

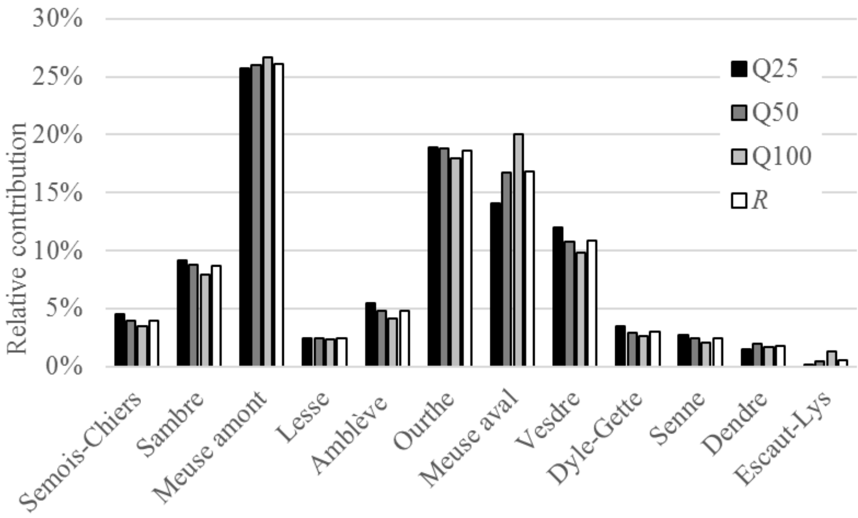

Figure 7: The relative contribution of each subbasin to the total flood damages and to the flood risk indicator (*R*) for the baseline scenario (2010 land use map).

3.3.2 Influence of the urbanization scenarios on the magnitude of the total flood risk indicator

In this section, we compare the influence of the spatial planning policies on the increase in the value of the flood risk indicator for the 2050 time horizon compared with the baseline scenario.

Table 4 shows that the increase in the total flood risk indicator ranges between 0% and 44% depending on the spatial planning scenario for a high demand rate, and between 0% and 22% for a low demand rate. Banning new developments in flood-prone zones is by far the most influential spatial planning factor. A ban on new developments in flood-prone zone 3 would limit the increase in the flood risk indicator to roughly one-third of the values without any ban on new developments. Extending the ban to flood prone-zones 2 reduces the increase in flood risk indicator to only 1-2% when compared with the baseline scenario. Banning new developments in all flood-prone zones leads to no increase in flood damages for the computed flood discharges because their maximum inundation extents match the maximum flood-prone zones. The effects of urban development restrictions in flood-prone zones on the increase in flood damage are of the same magnitude for both BAU and densification strategies.

In all cases, densification spatial planning policy leads to a higher flood risk indicator compared to BAU, especially in the case where no or moderate urban development restrictions are adopted in flood-prone zones. This is quite logical because the urban areas where densification may occur are predominantly located in valleys in Wallonia, following the pattern inherited from the industrial revolution. Without banning new developments or with a regulation in flood-prone zones 3, the rise in the flood risk indicator is respectively from 9 to 15 percentage and from 2 to 3 percentage points higher in the densification scenario. Basically, this means that densification policies designed to curb sprawl should be accompanied by adequate restriction measures in flood-prone zones to mitigate the increased flood risk.

The influence of uncertainty related to the demand rate is lower than the effect of spatial planning policies. However, its impact remains significant because the increase in the flood risk indicator for a low urbanization rate scenario without regulation on new developments (with regulation in flood-prone zones 3) is 7 to 13 (2 to 3) percentage lower than that obtained with a high demand rate scenario.

Table 4: Increase in the flood risk indicator for 2050 based on different urbanization scenarios, compared with the baseline scenario (2010).

Spatial planning policy		**Demand rate for new development**		
Expansion vs. Densification	Urban development restrictions	High demand rate	Medium demand rate	Low demand rate
Business-as-usual (BAU)	None	29%	27%	22%
	In flood-prone zones 3	9%	8%	7%
	In flood-prone zones 2 and 3	1%	2%	1%
	In all flood-prone zones	0%	0%	0%
Densification	None	44%	37%	31%
	In flood-prone zones 3	12%	11%	9%
	In flood-prone zones 2 and 3	2%	2%	2%
	In all flood-prone zones	0%	0%	0%

3.3.3 Influence of the urbanization scenarios on the distribution of the flood risk indicator

The flood risk indicator in 2050 is strongly influenced by the spatial planning scenario (Table 4). In this section, we investigate the distribution of the increase in flood risk indicator among the subbasins depending on the spatial planning policy.

Figure 8-a indicates that in BAU scenarios, the demand rate poorly impacts the distribution of the increase in flood risk indicator between the subbasins. In contrast, the distribution of the flood risk indicator is highly influenced by the spatial planning approach. With no restriction on urban development in flood-prone zones, densification policy would lead to significant increases in flood damage when compared with BAU policy in the Meuse district (Figure 8-a). By contrast, a small reduction of the flood damage would be observed in the Escaut district.

In all subbasins, banning new developments in flood-prone zones 3 (Figure 8-b) has a high impact on the mitigation of the increase in the flood risk indicator (a reduction from 4.8×10^6 € to 1.4×10^6 €). Extending the ban to flood-prone zone 2 leads to a negligible increase in the flood risk indicator compared to 2010 in most sub-basins (rise in flood risk indicator reduced to around 3×10^5 €). Only for the Meuse amont, Meuse aval and Dyle-Gette subbasins, a significant additional mitigation of the flood risk indicator can be obtained by an extension of the banning on new development in flood-prone zones 1 (a reduction of 2.5×10^5 € for the increased flood risk indicator over the three subbasins).

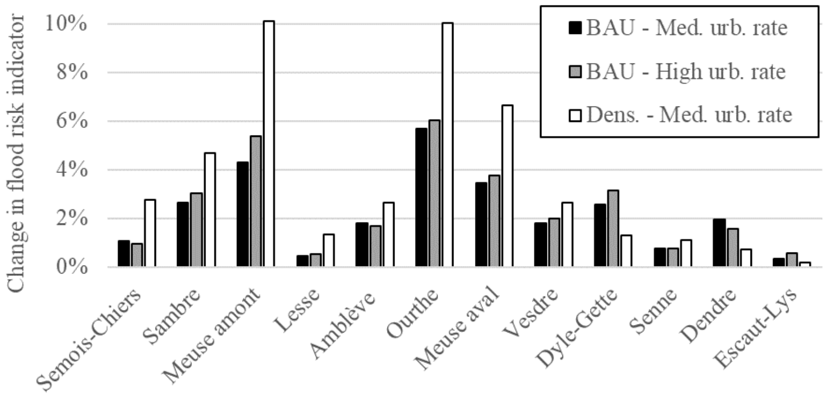

(a)

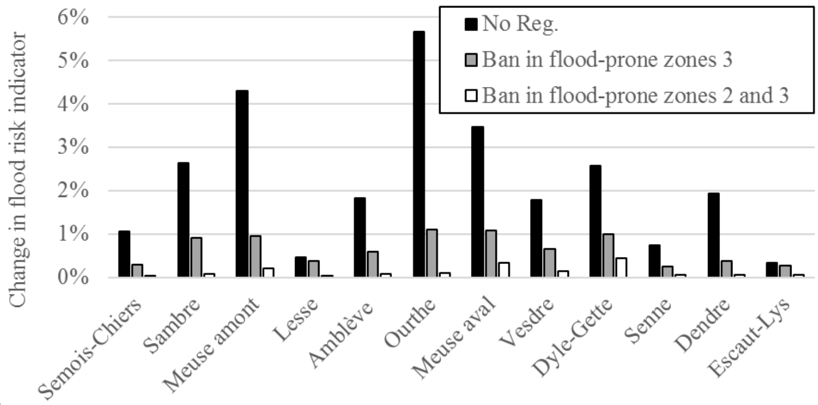

(b)

Figure 8: Changes in the values of the flood risk indicator in 2050 for each subbasin compared to the total flood risk indicator for the baseline scenario considering a business-as-usual scenario with (a) all demand rates and (b) medium demand rate with and without ban regulations on urbanization in flood-prone zones.

3.4. Increase in flood risk indicator for different future time-horizons

In this section, the increase in flood risk indicator is quantified for each decade until 2100 (Table 5). The change rate of the total increase in flood risk indicator remains broadly constant over the decades for the different future time horizons.

Table 5: Increase in the flood risk indicator per decade in Wallonia.

Spatial planning policy		**Demand rate for new development**	
Expansion vs. Densification	Urban development restrictions	High demand rate	Low demand rate
Business-as-usual	None	7.5%	5.5%
	In flood zones 3	-	2%
	In flood zones 2 and 3	-	1%
	In all flood zones	-	0%
Densification	None	11%	-

The first three scenarios are representative of the range of variation of the computed flood risk indicator without restrictions on urbanization in flood-prone zones. The comparison of the last three scenarios with the first enables to assess the effect of restrictions on new developments in flood prone-zones.

The distribution of changes in the flood risk indicator between the different subbasins is slightly affected by the time horizon. The variations of the relative contribution of a subbasin to the total flood risk indicator at the time horizon 2100 are the highest for the first urbanization scenario (BAU with a low urbanization rate and no regulation on new urbanization), in which the maximum change of the relative contribution is -4% points (Meuse amont subbasins) while the average absolute change is as low as 1.3% points.

4. Conclusions

This paper investigated the effects of different spatial planning policies on future flood risks in Wallonia (Belgium) for flood discharges corresponding to return periods of 25, 50, and 100 years. A number of future urban patterns were generated with a spatial ABM considering several factors. This model simulated both urban expansion and densification. An important contribution of this study is the consideration of urban density and not just binary data (urban/nonurban) in the estimation of flood damage. Our results revealed that the estimation of flood damage may be overestimated by 48% to 105% when models do not take into consideration urban density.

The uncertainty related to the demand for future urban development strongly influenced the computed flood damages and their spatial distribution. Without considering any ban on urban development in flood-prone zones, the increase in total flood risk varies by a factor of approximately two depending on the urbanization scenario. Quite importantly, the sensitivity of the computed rise in flood damage to the spatial planning policy (BAU vs. densification) is shown to be much higher than to the demand rate. This highlights that spatial policies may have a substantial influence on future flood risk, even for a fixed demand rate.

For the future time horizons 2030 to 2100, the increase in flood risk is expected to be between 5.5% and 11% per decade compared with the situation in 2010. Banning new developments in flood-prone zones would enable a strong reduction of expected increases. They would be reduced by a factor of three with a ban on new developments in flood-prone zone 3 (high flood hazard) and to values lower than 1% with an extension of the ban to other flood-prone zones, regardless of the spatial planning policy.

It is worth mentioning that the coarse resolution, 100 m², of the land use maps and the assumption that flow characteristics do not change with urbanization are two limitations of this study. Furthermore, it should be stressed that the results of the present study are specific to a given territory where existing urban zones are somehow concentrated in flood-prone zones. The results may differ in those places where urban settlements did not initially develop along water channels. Nonetheless, we believe that the main findings of this research are significantly relevant contributions to sustainable flood risk management that pave the way for more flood-proof and resilient spatial planning. One of the significant findings of the current study for urban planners is that a spatial planning policy oriented towards densification without expansion should be accompanied by appropriate mitigation measures, either at the site or at the building scale (e.g. Bruwier et al., 2018).

Acknowledgements: The research was funded through the ARC grant for Concerted Research Actions for project number 13/17-01 financed by the French Community of Belgium (Wallonia-Brussels Federation) and through the European Regional Development Fund – FEDER (Wal-e-Cities Project). The authors would like to thank the anonymous reviewers and the editors for insightful comments that led to substantial improvements over the earlier version of this paper.

References

Achleitner, S., Huttenlau, M., Winter, B., Reiss, J., Plörer, M., Hofer, M., 2016. Temporal development of flood risk considering settlement dynamics and local flood protection measures on catchment scale: an Austrian case study. Int. J. River Basin Manag. 14, 273–285. https://doi.org/10.1080/15715124.2016.1167061

Beckers, A., Dewals, B., Erpicum, S., Dujardin, S., Detrembleur, S., Teller, J., Pirotton, M., Archambeau, P., 2013. Contribution of land use changes to future flood damage along the river Meuse in the Walloon region. Nat Hazards Earth Syst Sci 13, 2301–2318. https://doi.org/10.5194/nhess-13-2301-2013

Bruwier, M., Erpicum, S., Pirotton, M., Archambeau, P., Dewals, B.J., 2015. Assessing the operation rules of a reservoir system based on a detailed modelling chain. Nat Hazards Earth Syst Sci 15, 365–379. https://doi.org/10.5194/nhess-15-365-2015

Bruwier, M., Mustafa, A., Aliaga, D.G., Archambeau, P., Erpicum, S., Nishida, G., Zhang, X., Pirotton, M., Teller, J., Dewals, B., 2018. Influence of urban pattern on inundation flow in floodplains of lowland rivers. Sci. Total Environ. 622–623, 446–458. https://doi.org/10.1016/j.scitotenv.2017.11.325

Büchele, B., Kreibich, H., Kron, A., Thieken, A., Ihringer, J., Oberle, P., Merz, B., Nestmann, F., 2006. Flood-risk mapping: contributions towards an enhanced assessment of extreme events and associated risks. Nat. Hazards Earth Syst. Sci. 6, 485–503.

Cammerer, H., Thieken, A.H., Verburg, P.H., 2013. Spatio-temporal dynamics in the flood exposure due to land use changes in the Alpine Lech Valley in Tyrol (Austria). Nat. Hazards 68, 1243–1270. https://doi.org/10.1007/s11069-012-0280-8

Ernst, J., Dewals, B.J., Detrembleur, S., Archambeau, P., Erpicum, S., Pirotton, M., 2010. Micro-scale flood risk analysis based on detailed 2D hydraulic modelling and high resolution geographic data. Nat. Hazards 55, 181–209. https://doi.org/10.1007/s11069-010-9520-y

García, A.M., Santé, I., Boullón, M., Crecente, R., 2013. Calibration of an urban cellular automaton model by using statistical techniques and a genetic algorithm. Application to a small urban settlement of NW Spain. Int. J. Geogr. Inf. Sci. 27, 1593–1611. https://doi.org/10.1080/13658816.2012.762454
Han, Y., Jia, H., 2016. Simulating the spatial dynamics of urban growth with an integrated modeling approach: A case study of Foshan, China. Ecol. Model. https://doi.org/10.1016/j.ecolmodel.2016.04.005
Hannaford, J., 2015. Climate-driven changes in UK river flows: A review of the evidence. Prog. Phys. Geogr. Earth Environ. 39, 29–48. https://doi.org/10.1177/0309133314536755
Huong, H.T.L., Pathirana, A., 2013. Urbanization and climate change impacts on future urban flooding in Can Tho city, Vietnam. Hydrol Earth Syst Sci 17, 379–394. https://doi.org/10.5194/hess-17-379-2013
IPCC, 2014. Climate Change 2014: Synthesis Report. Contribution of Working Groups I, II and III to the Fifth Assessment Report of the Intergovernmental Panel on Climate Change.
Jenks, G.F., Caspall, F.C., 1971. Error on Choroplethic Maps: Definition, Measurement, Reduction. Ann. Assoc. Am. Geogr. 61, 217–244. https://doi.org/10.1111/j.1467-8306.1971.tb00779.x
Kreibich, H., Piroth, K., Seifert, I., Maiwald, H., Kunert, U., Schwarz, J., Merz, B., Thieken, A.H., 2009. Is flow velocity a significant parameter in flood damage modelling? Nat Hazards Earth Syst Sci 9, 1679–1692. https://doi.org/10.5194/nhess-9-1679-2009
Kreibich, H., Seifert, I., Merz, B., Thieken, A.H., 2010. Development of FLEMOcs – a new model for the estimation of flood losses in the commercial sector. Hydrol. Sci. J. 55, 1302–1314. https://doi.org/10.1080/02626667.2010.529815
Long, Y., Han, H., Lai, S.-K., Mao, Q., 2013. Urban growth boundaries of the Beijing Metropolitan Area: Comparison of simulation and artwork. Cities 31, 337–348. https://doi.org/10.1016/j.cities.2012.10.013
Löschner, L., Herrnegger, M., Apperl, B., Senoner, T., Seher, W., Nachtnebel, H.P., 2017. Flood risk, climate change and settlement development: a micro-scale assessment of Austrian municipalities. Reg. Environ. Change 17, 311–322. https://doi.org/10.1007/s10113-016-1009-0
Matthews, R.B., Gilbert, N.G., Roach, A., Polhill, J.G., Gotts, N.M., 2007. Agent-based land-use models: a review of applications. Landsc. Ecol. 22, 1447–1459.
Merz, B., Thieken, A.H., Gocht, M., 2007. Flood Risk Mapping At The Local Scale: Concepts and Challenges, in: Flood Risk Management in Europe, Advances in Natural and Technological Hazards Research. Springer, Dordrecht, pp. 231–251. https://doi.org/10.1007/978-1-4020-4200-3_13
Moel, H. de, Aerts, J.C.J.H., 2010. Effect of uncertainty in land use, damage models and inundation depth on flood damage estimates. Nat. Hazards 58, 407–425. https://doi.org/10.1007/s11069-010-9675-6
Mustafa, A., Cools, M., Saadi, I., Teller, J., 2017. Coupling agent-based, cellular automata and logistic regression into a hybrid urban expansion model (HUEM). Land Use Policy 69C, 529–540. https://doi.org/10.1016/j.landusepol.2017.10.009
Mustafa, A., Heppenstall, A., Omrani, H., Saadi, I., Cools, M., Teller, J., 2018a. Modelling built-up expansion and densification with multinomial logistic regression, cellular automata and genetic algorithm. Comput. Environ. Urban Syst. 67, 147–156. https://doi.org/10.1016/j.compenvurbsys.2017.09.009
Mustafa, A., Rompaey, A.V., Cools, M., Saadi, I., Teller, J., 2018b. Addressing the determinants of built-up expansion and densification processes at the regional scale. Urban Stud. 0042098017749176. https://doi.org/10.1177/0042098017749176
Mustafa, A., Saadi, I., Cools, M., Teller, J., 2018c. A Time Monte Carlo method for addressing uncertainty in land use change models. Int. J. Geogr. Inf. Sci. https://doi.org/10.1080/13658816.2018.1503275
Poelmans, L., Rompaey, A.V., Ntegeka, V., Willems, P., 2011. The relative impact of climate change and urban expansion on peak flows: a case study in central Belgium. Hydrol. Process. 25, 2846–2858. https://doi.org/10.1002/hyp.8047
Poelmans, L., Van Rompaey, A., Batelaan, O., 2010. Coupling urban expansion models and hydrological models: How important are spatial patterns? Land Use Policy 27, 965–975. https://doi.org/10.1016/j.landusepol.2009.12.010
Tang, Z., Engel, B.A., Pijanowski, B.C., Lim, K.J., 2005. Forecasting land use change and its environmental impact at a watershed scale. J. Environ. Manage. 76, 35–45. https://doi.org/10.1016/j.jenvman.2005.01.006
UNISDR, 2009. 2009 UNISDR terminology on disaster risk reduction.
Wang, H., He, S., Liu, X., Dai, L., Pan, P., Hong, S., Zhang, W., 2013. Simulating urban expansion using a cloud-based cellular automata model: A case study of Jiangxia, Wuhan, China. Landsc. Urban Plan. 110, 99–112. https://doi.org/10.1016/j.landurbplan.2012.10.016
White, R., Engelen, G., 2000. High-resolution integrated modelling of the spatial dynamics of urban and regional systems. Comput. Environ. Urban Syst. 24, 383–400. https://doi.org/10.1016/S0198-9715(00)00012-0

Appendices

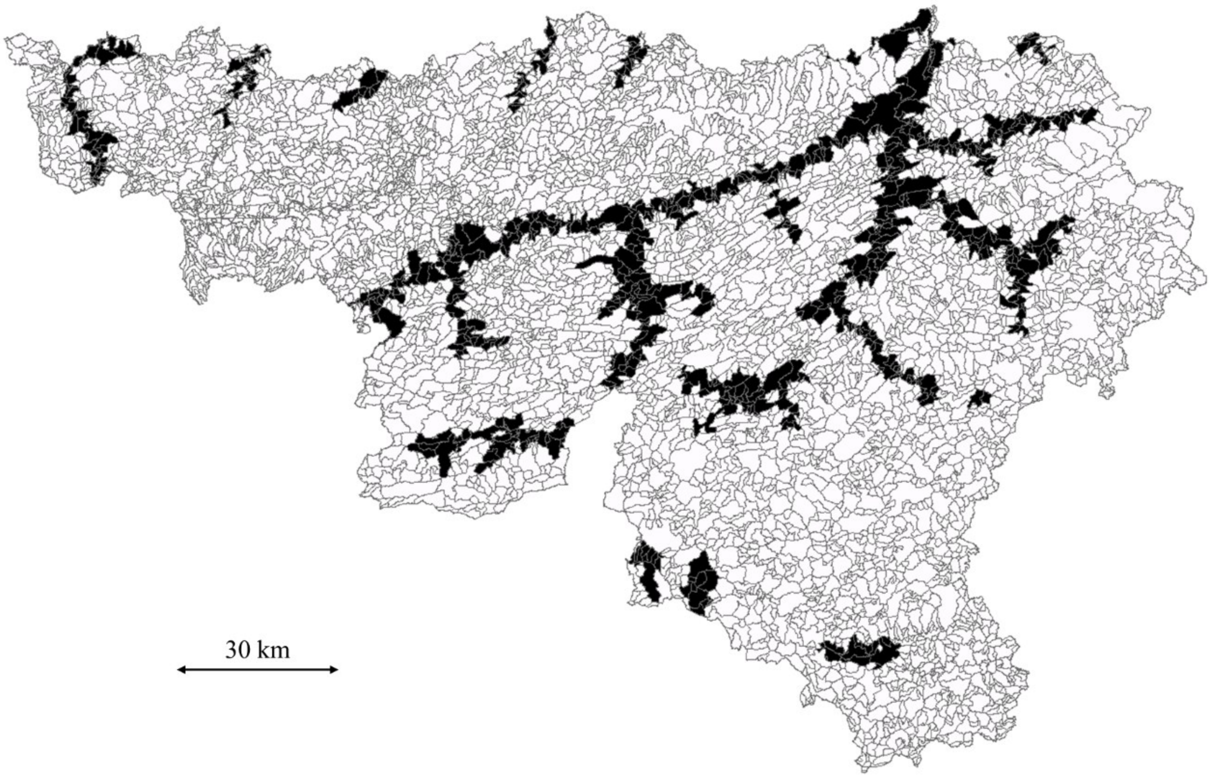

Figure A-1: Hydrographic sectors for which computations were performed by the HECE in the context of the preparation of flood hazard maps.

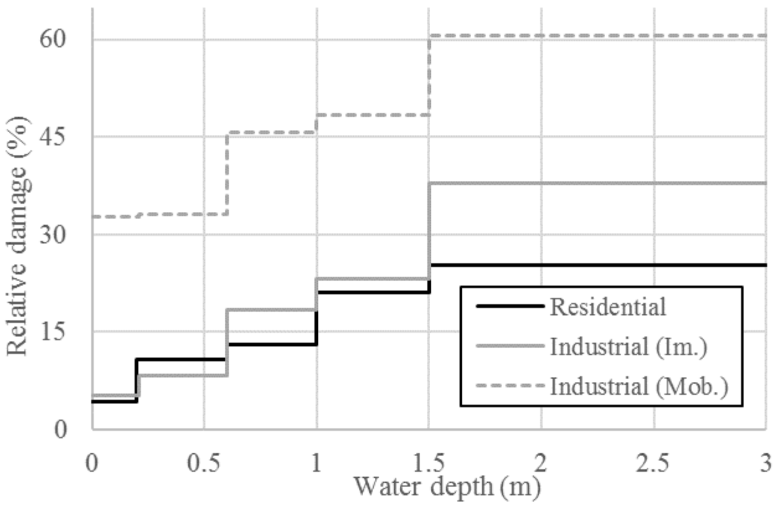

Figure A-2: FLEMO stage-damage functions for residential and industrial land use categories.

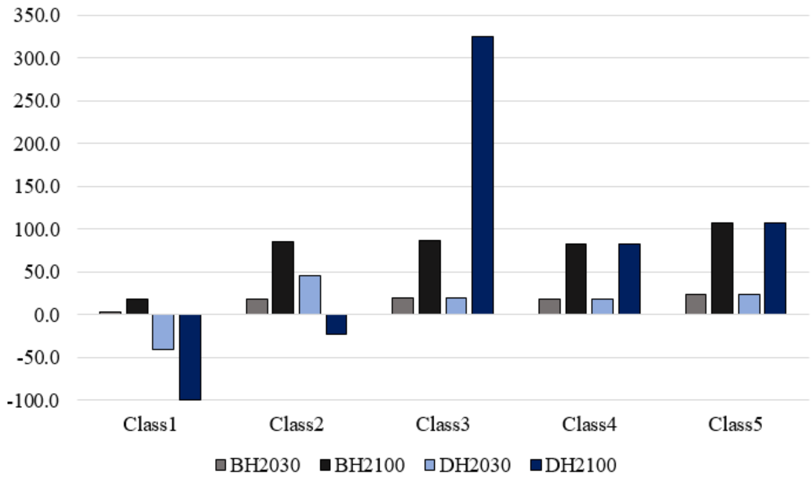

Figure A-3*:* Change rate (%) of the area of each urban class related to its area in 2010.